Susceptibility-Weighted Imaging. Initial Experience

José Luis Ascencio L.[1]; Tania Isabel Ruiz Z.[2]

[1] Escanografia Neurologica, Medellin, Colombia
[2] Universidad CES, Radiology, Medellín, Antioquia, Colombia

Introduction

Susceptibility-weighted imaging (SWI) is a sequence that utilizes a phenomenon in which the phase and change in the local magnetic field of the tissues are proportional to one another, provided the echo time is constant [1]. It uses magnitude and phase images, as well as a summation of these in a three-dimensional gradient echo sequence with flow compensation [2]. It offers very high sensitivity for visualizing calcium, non-heme iron (ferritin) and hemoglobin degradation products (deoxyhemoglobin and hemosiderin) [3, 4].

Initial experience

By means of a series of cases we will illustrate the clinical usefulness of SWI with certain neurological conditions. The studies reviewed were performed in the Neurological Scanography Magnetic Resonance Imaging Service using a Siemens MAGNETOM ESSENZA 1.5 Tesla MRI unit with the following settings: TR 49 ms, TE 40 ms, FA 15°, number of slices 60, slice thickness 2 mm, acquisition matrix 256 ×157.

Susceptibility-weighted imaging takes advantage of the loss of signal intensity created by alterations in a homogenous magnetic field; these disturbances can be caused by several different paramagnetic or diamagnetic substances. The loss of signal intensity in the T2*-weighted sequence is a result of the difference in the precession rate of the spins [5].

The susceptibility image is obtained during the acquisition process by combining the magnitude and phase of the images. Routine MR images are magnitude images where the signal's intensity is converted to a gray scale. Phase information is obtained at the same time, but is generally ignored. A filter is applied to the phase image (High-pass Hamming Window Filter) on a 64 × 64 matrix to reduce aliasing artifacts. A new phase mask is created which, when added to the magnitude image, creates the susceptibility image. In order to obtain a better interpretation, minimum intensity projections (minIP) are used [6]. During post-processing the phase contrast image is filtered to reduce undesirable low spatial frequency components, leaving the high frequency field variations. The phase mask created can be 'positive' or 'negative'. The phase mask is multiplied using the original magnitude image to produce images that maximize the negative intensity of the mineralization of the parenchyma. Minimum intensity projection (usually from 2 to 4 slices) is used to display the processed data [1].

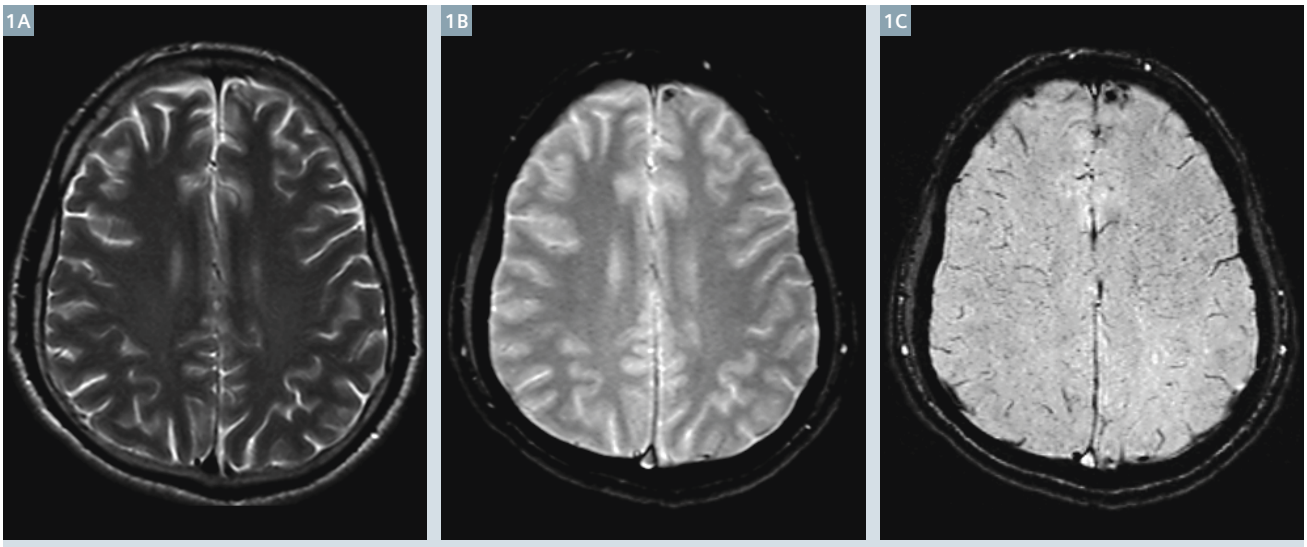

1 Patient with bilateral frontal hemorrhagic contusion. **(1A)** T2w axial; no lesions observed. **(1B)** Axial gradient echo shows a low-signal lesion in left frontal lobe with a slight blooming effect. **(1C)** SWI magnitude, two bilateral frontal hemorrhagic contusions are observed.

The method is highly sensitive for purposes of visualizing venous circulation, blood products and iron content, and is also useful for evaluating the vascularization of tumors and for identifying brain tissue that has been compromised by a stroke, vascular dementia or trauma, and can also be used in functional imaging [1, 4, 7-9] (Fig. 1).

Hemorrhage

Oxyhemoglobin, formed by the binding of an oxygen and an iron atom contained in the Hem group, is a diamagnetic substance. When the oxygen is released from the iron atom it forms deoxyhemoglobin, which is paramagnetic because of its unpaired electrons. Metahemoglobin is produced when deoxyhemoglobin oxidizes, making it less stable; in this state there is little susceptibility effect and thus it is more easily visualized in T1w images. Hemosiderin is the final product of the degradation of hemoglobin when it degrades within phagocytic cells, and is a highly paramagnetic [3, 4, 10] substance. Diamagnetic substances produce a weak local magnetic field, while paramagnetics generate a stronger magnetic field that leads to a signal de-phase and therefore a signal reduction in the T2*w sequence [4]. The ferritin produced by different metabolic processes also has paramagnetic characteristics and is associated with Parkinson's disease, Huntington's disease and Alzheimer's disease [9-11].

Trauma

In the detection of diffuse axonal damage, this approach is more sensitive than conventional imaging for detecting microhemorrhages in the deep and subcortical white matter, which can be obscured in computed tomography (CT) scans [12, 13]. It is three to six times more sensitive than gradient echo images for detecting the number, size, and location of the lesions associated with this clinical status of the patient [1, 13-16]. It is equally useful in detecting brainstem lesions, subarachnoid and intraventricular hemorrhage, as well as other types of hemorrhagic lesions of different origins [17] (Fig. 2).

Calcifications

Calcium is also diamagnetic and can lead to changes in the susceptibility image [12, 18]. SWI differentiates iron from calcium based on their diamagnetic or paramagnetic characteristics in the filtered-phase image. Calcium appears brilliant in this latter image, while the hemorrhage and its derivative products have low signal intensity. This differentiation is important when dealing with neurodegenerative and metabolic diseases, trauma, and tumors [12, 18].

Vascular malformations

Venous blood causes non-homogeneity in the magnetic field due to the paramagnetic effect of the deoxygenated blood due to T2* reduction, depending on the oxygen saturation, the hematocrit and the condition of the erythrocytes; thus, the deoxyhemoglobin present in venous blood allows for the visualization of the latter [4] as well as the phase difference between the vessels and surrounding structures [19]. The susceptibility image provides contrast similar to that of a functional image (BOLD blood oxygen level-dependent).

SWI is more sensitive in the detection of vascular structures that are hidden to T2* and low-flow malformations that are not detected by MR angiography, such as venous development malformations, telangiectasias and cavernomas, as well as vascular abnormalities and calcifications related to Sturge-Weber Syndrome, since it is not affected by flow velocity or direction [20-24]. In dural sinus thrombosis they show venous statis and collateral flow, as well as early detection of venous hypertension before infarcts or hemorrhages occur [7, 8, 19] (Figs. 3–5).

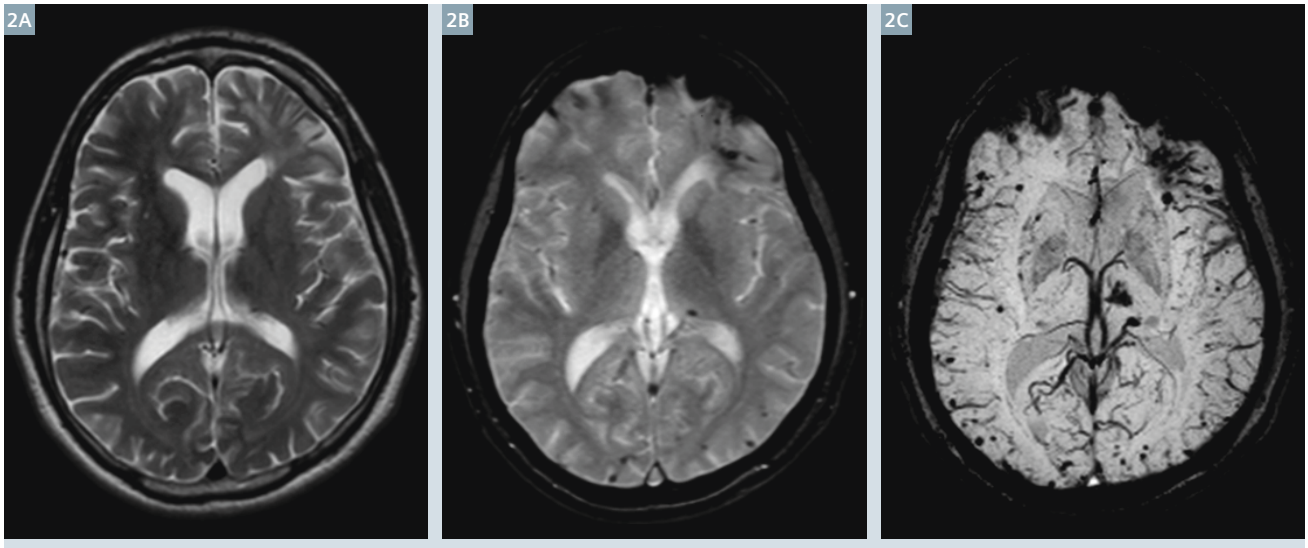

2 Patient with diffuse axonal lesion. **(2A)** T2w axial; no lesions observed. **(2B)** Low-signal, puntiform lesions. **(2C)** SWI minIP makes the multiple microhemorrhagic lesions more apparent.

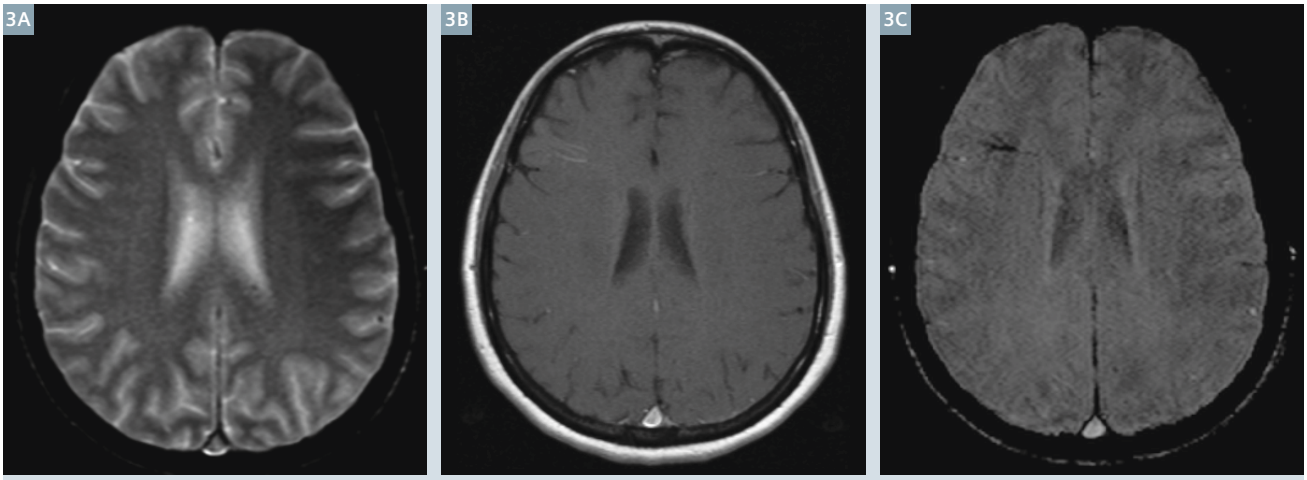

3 Venous development anomaly. **(3A)** Axial gradient echo; anomaly not visible. **(3B)** Axial contrast-enhanced image shows right frontal venous development anomaly that is more evident in the susceptibility image **(3C)**.

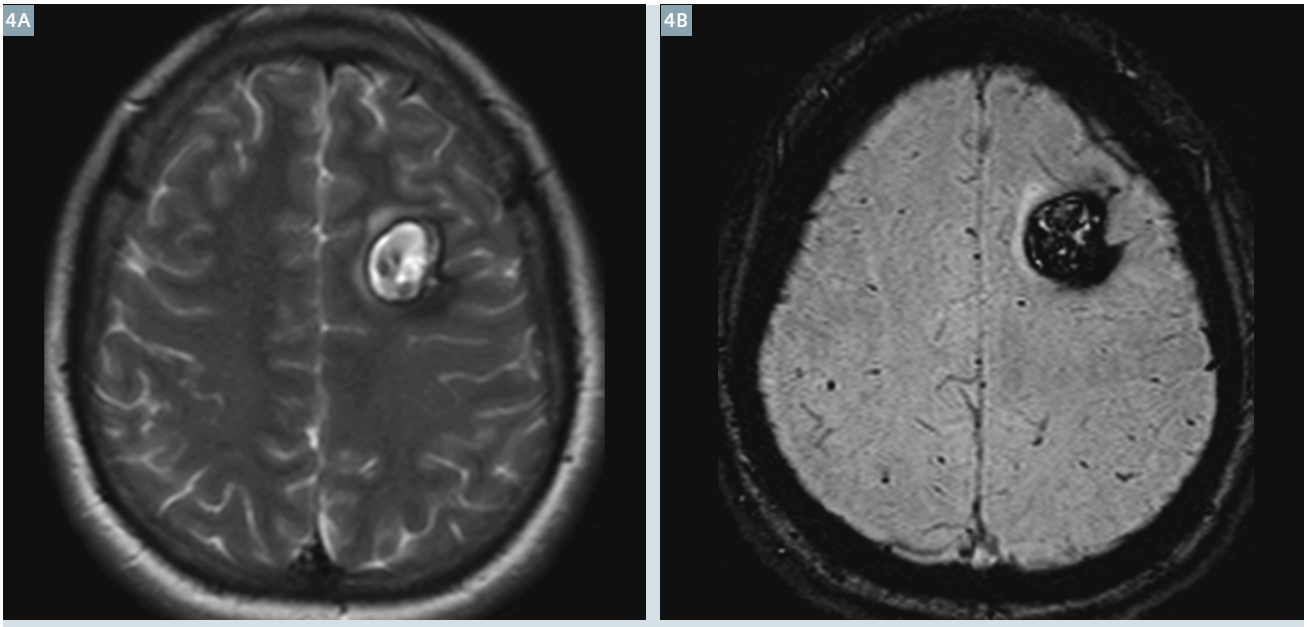

4 Left frontal cavernoma. **(4A)** Axial proton density-weighted image; **(4B)** minIP SWI.

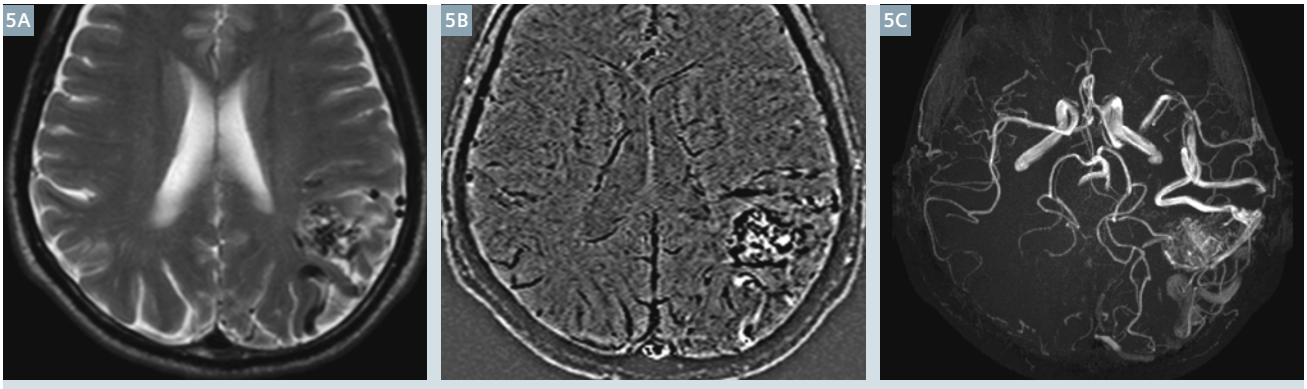

5 Left parietal arteriovenous malformation. **(5A)** Axial PDw show serpinginous images with absence of flow signal. **(5B)** mIP SWI. **(5C)** MIP TOF shows the AVM and the cortical drainage vein.

Brain tumors

This approach provides information that supplements T1 with contrast for detecting margins, internal architecture, hemorrhage and vascularization of a tumor that are not visible with conventional sequences. This aids in differentiating between a recurring tumor and post-operative changes. The use of susceptibility imaging before and after the administration of gadolinium can differentiate areas of enhancement of the vessels. Because of its suppression of cerebrospinal fluid, it enhances contrast between edema and normal tissue, similarly to what is provided by FLAIR, thus facilitating the detection of space-occupying lesions [4, 7, 25] (Figs. 6–8).

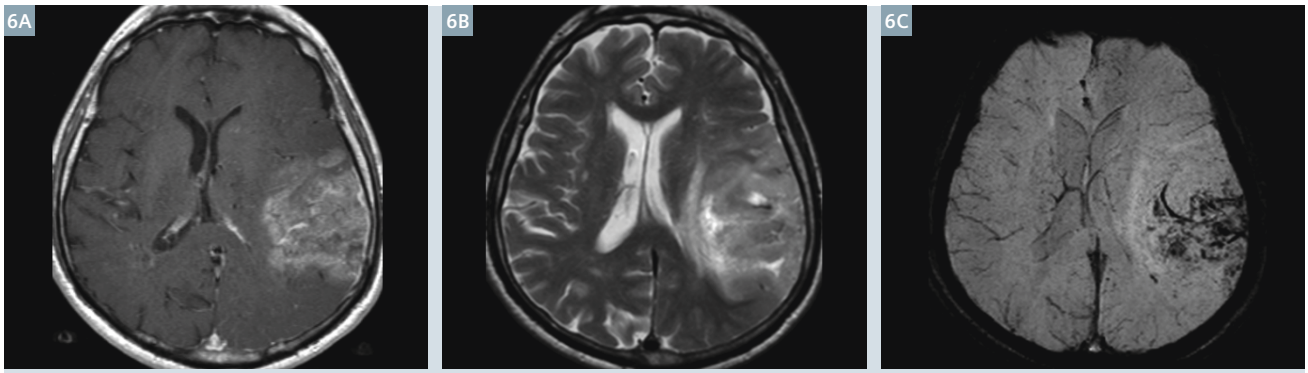

6 Hemorrhagic metathesis. **(6A)** T1w axial gadolinium-enhanced, **(6B)** T2w axial show a left parietal mass with heterogeneous enhancement, perilesional edema and mass effect on the lateral ventricles. **(6C)** MIP SWI shows hypervascularity and hemorrhage in the interior of the mass.

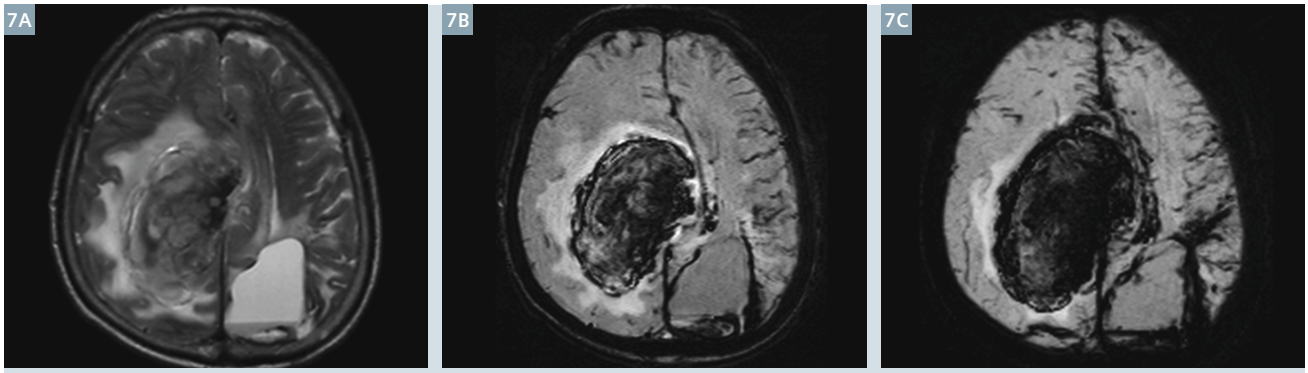

7 Metastatic melanoma. **(7A)** T2w axial; large mass displacing the midline, with major edema and hypointense zone due to hemorrhage in the medial portion. **(7B)** Magnitude image, **(7C)** MIP SWI shows a greater hemorrhagic component of the mass, on the contralateral side, as well as intraventricular hemorrhaging.

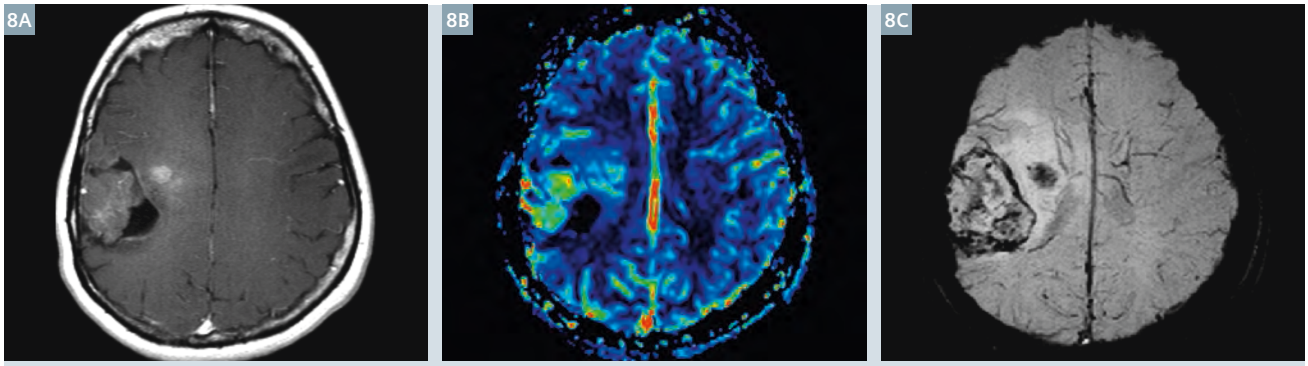

8 Oligodendroglioma. **(8A)** T1w axial gadolinium shows mass with enhanced foci and a cystic component, **(8B)** MIP SWI right parietal hypervascular mass with increased relative flow **(8C)**.

Cerebrovascular disease

The susceptibility image can be used together with diffusion images to detect the hypoperfused region, the presence of hemorrhaging within the infarct (which could affect the treatment), detect acute thrombus and predict the likelihood of hemorrhagic transformation and hemorrhagic complications during and after thrombolysis treatment, as well as microbleeding due to amyloid angiopathy and lacunar infarcts in patients with hypertensive encephalopathy [19, 26-28] (Figs. 9, 10).

Vascular occlusion can change the susceptibility of the tissue as a result of reduced arterial flow and an increase in the accumulation of deoxygenated blood, which increases the amount of deoxyhemoglobin that can be detected by SWI [27, 29].

Neurodegenerative illnesses

Certain disorders, such as Parkinson's Disease, Huntington's Disease, Alzheimer's, multiple sclerosis and amyotrophic lateral sclerosis (Lou Gherig's Disease) present with abnormal iron deposition, which can be detected and quantified using susceptibility imaging [11, 30-33]. SWI can show chronic demyelinating plaques with iron depositions that are hidden in conventional sequences, as the iron content makes the lesions more visible. It can also determine the iron content of the nucleii of deep gray matter that can also be observed in patients with multiple sclerosis, as well as the perivenular distribution of the demyelinating lesions [30].

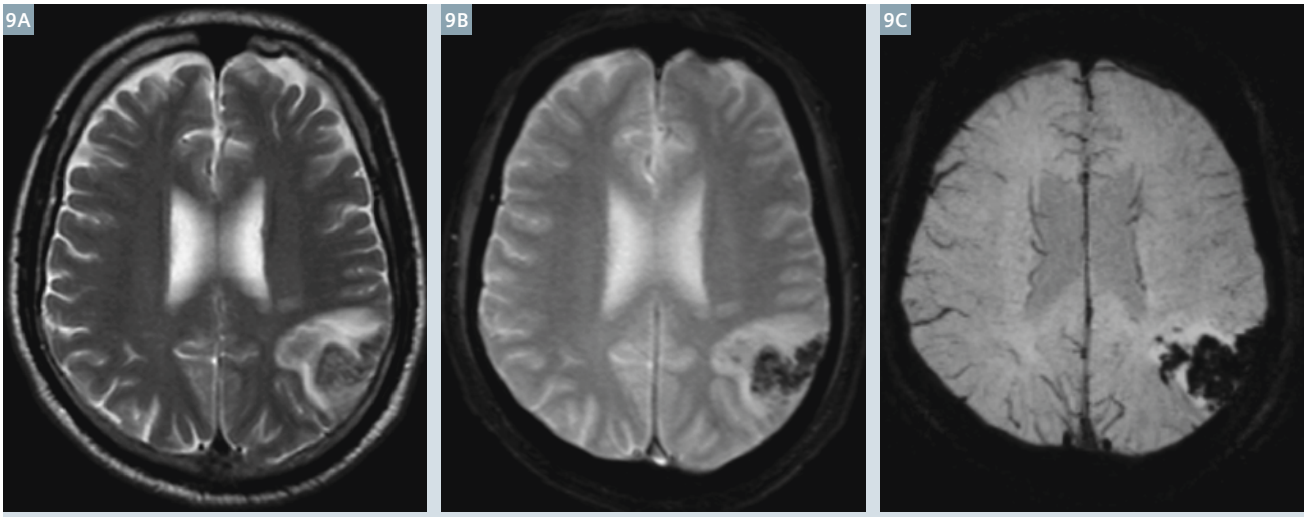

9 CVD with hemorrhagic transformation. **(9A)** Axial T2w, **(9B)** gradient echo in patient with left parietal hemorrhagic infarct with surrounding edema and hemorrhage. **(9C)** SWI makes the greater hemorrhagic component more obvious.

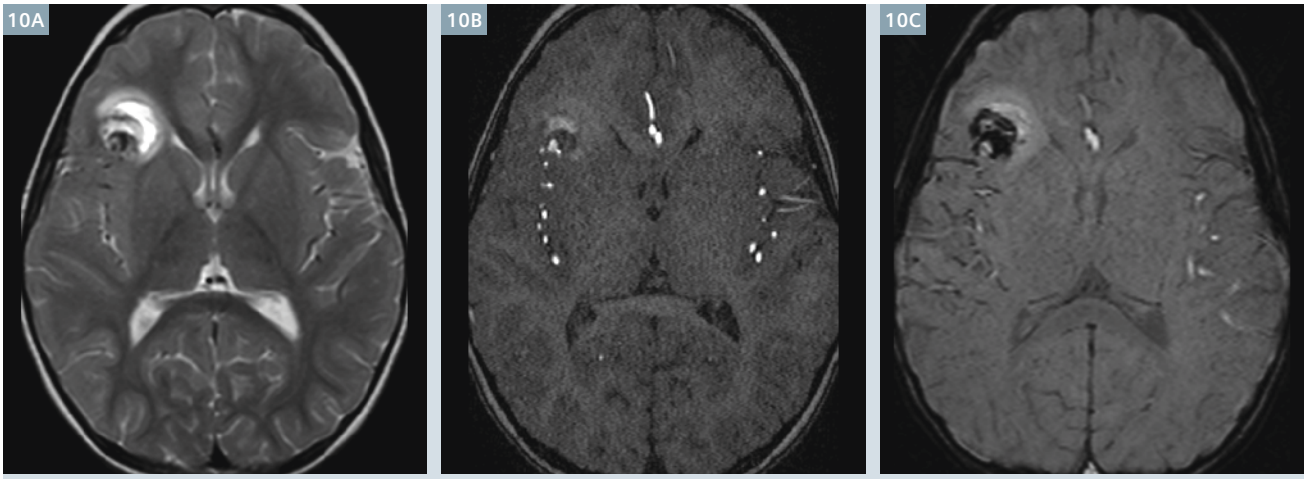

10 Right MCA aneurism with bleeding. **(10A)** Axial T2w, **(10B)** TOF demonstrating aneurysm with bleeding, **(10C)** SWI aneurism with greater bleeding than that shown in the T2w sequence.

References

1 Haacke EM, Xu Y, Cheng Y-CN, Reichenbach JR. Susceptibility weighted imaging (SWI). Magnetic Resonance in Medicine. 2004;52(3):612-8.
2 Haacke EM, Mittal S, Wu Z, Neelavalli J, Cheng Y-CN. Susceptibility-Weighted Imaging: Technical Aspects and Clinical Applications, Part 1. AJNR Am J Neuroradiol. 2009 January 1, 2009;30(1):19-30.
3 Mittal S, Wu Z, Neelavalli J, Haacke EM. Susceptibility-Weighted Imaging: Technical Aspects and Clinical Applications, Part 2. AJNR Am J Neuroradiol. 2009 February 1, 2009;30(2):232-52.
4 Sehgal V, Delproposto Z, Haacke EM, Tong KA, Wycliffe N, Kido DK, et al. Clinical applications of neuroimaging with susceptibility-weighted imaging. Journal of Magnetic Resonance Imaging. 2005;22(4):439-50.
5 Tong KA, Ashwal S, Obenaus A, Nickerson JP, Kido D, Haacke EM. Susceptibility-Weighted MR Imaging: A Review of Clinical Applications in Children. AJNR Am J Neuroradiol. 2008 January 1, 2008;29(1):9-17.
6 Matsushita T AD, Arioka T, Inoue S, Kariya Y, Fujimoto M, Ida K, Sasai N, Kaji M, Kanazawa S, Joja I. Basic study of susceptibility-weighted imaging at 1.5T. Acta medica Okayama. [Journal Article]. 2008 Jun;62(3):159-68.
7 Thomas B, Somasundaram S, Thamburaj K, Kesavadas C, Gupta A, Bodhey N, et al. Clinical applications of susceptibility weighted MR imaging of the brain – a pictorial review. Neuroradiology. 2008;50(2):105-16.
8 Ong BC, Stuckey SL. Susceptibility weighted imaging: A pictorial review. Journal of Medical Imaging and Radiation Oncology. 2010;54(5):435-49.
9 Robinson RJ, Bhuta S. Susceptibility-Weighted Imaging of the Brain: Current Utility and Potential Applications. Journal of Neuroimaging. 2011:no-no.
10 Goos JDC, van der Flier WM, Knol DL, Pouwels PJW, Scheltens P, Barkhof F, et al. Clinical Relevance of Improved Microbleed Detection by Susceptibility-Weighted Magnetic Resonance Imaging. Stroke. 2011 May 12, 2011:STROKEAHA. 110.599837.
11 Gupta D, Saini J, Kesavadas C, Sarma P, Kishore A. Utility of susceptibility-weighted MRI in differentiating Parkinson's disease and atypical parkinsonism. Neuroradiology. 2010;52(12):1087-94.
12 ZHU Wen-zhen QJ-p, ZHAN Chuan-jia, SHU Hong-ge, ZHANG Lin, WANG Cheng-yuan, XIA Li-ming, HU Jun-wu, FENG Ding-yi. Magnetic resonance susceptibility weighted imaging in detecting intracranial calcification and hemorrhage. Chinese Medical Journal. [Journal Article]. 2008 oct 20;121(20):2021-5.
13 Beauchamp MH, Ditchfield M, Babl FE, Kean M, Catroppa C, Yeates KO, et al. Detecting Traumatic Brain Lesions in Children: CT versus MRI versus Susceptibility Weighted Imaging (SWI). Journal of Neurotrauma. 2011;28(6):915-27.
14 Wang M, Dai Y, Han Y, Haacke EM, Dai J, Shi D. Susceptibility weighted imaging in detecting hemorrhage in acute cervical spinal cord injury. Magnetic resonance imaging. 2011;29(3):365-73.
15 Tong KA, Ashwal S, Holshouser BA, Shutter LA, Herigault G, Haacke EM, et al. Hemorrhagic Shearing Lesions in Children and Adolescents with Posttraumatic Diffuse Axonal Injury: Improved Detection and Initial Results1. Radiology. 2003 May 1, 2003;227(2):332-9.
16 Babikian T, Freier MC, Tong KA, Nickerson JP, Wall CJ, Holshouser BA, et al. Susceptibility weighted imaging: neuropsychologic outcome and pediatric head injury. Pediatr Neurol. 2005;33(3):184-94.
17 Wu Z, Li S, Lei J, An D, Haacke EM. Evaluation of Traumatic Subarachnoid Hemorrhage Using Susceptibility-Weighted Imaging. AJNR Am J Neuroradiol. 2010 August 1, 2010;31(7):1302-10.
18 Wu Z, Mittal S, Kish K, Yu Y, Hu J, Haacke EM. Identification of calcification with MRI using susceptibility-weighted imaging: A case study. Journal of Magnetic Resonance Imaging. 2009;29(1):177-82.
19 Tsui Y-K, Tsai FY, Hasso AN, Greensite F, Nguyen BV. Susceptibility-weighted imaging for differential diagnosis of cerebral vascular pathology: A pictorial review. Journal of the neurological sciences. 2009;287(1):7-16.
20 Hu J, Yu Y, Juhasz C, Kou Z, Xuan Y, Latif Z, et al. MR susceptibility weighted imaging (SWI) complements conventional contrast enhanced T1 weighted MRI in characterizing brain abnormalities of Sturge-Weber Syndrome. Journal of Magnetic Resonance Imaging. 2008;28(2):300-7.
21 Deistung A, Dittrich E, Sedlacik J, Rauscher A, Reichenbach JR. ToF-SWI: Simultaneous time of flight and fully flow compensated susceptibility weighted imaging. Journal of Magnetic Resonance Imaging. 2009;29(6):1478-84.
22 Koopmans P, Manniesing R, Niessen W, Viergever M, Barth M. MR venography of the human brain using susceptibility weighted imaging at very high field strength. Magnetic Resonance Materials in Physics, Biology and Medicine. 2008;21(1):149-58.
23 de Champfleur NM, Langlois C, Ankenbrandt WJ, Le Bars E, Leroy MA, Duffau H, et al. Magnetic Resonance Imaging Evaluation of Cerebral Cavernous Malformations With Susceptibility-Weighted Imaging. Neurosurgery. 2011;68(3):641-8 10.1227/NEU.0b013e31820773cf.
24 Jagadeesan BD, Delgado Almandoz JE, Moran CJ, Benzinger TLS. Accuracy of Susceptibility-Weighted Imaging for the Detection of Arteriovenous Shunting in Vascular Malformations of the Brain. Stroke. 2011 January 1, 2011;42(1):87-92.
25 Hori M, Ishigame K, Kabasawa H, Kumagai H, Ikenaga S, Shiraga N, et al. Precontrast and postcontrast susceptibility-weighted imaging in the assessment of intracranial brain neoplasms at 1.5 T. Japanese Journal of Radiology. 2010;28(4):299-304.
26 Cherian A, Thomas B, Kesavadas C, Baheti N, Wattamwar P. Ischemic hyperintensities on T1-weighted magnetic resonance imaging of patients with stroke: New insights from susceptibility weighted imaging2010 January 1, 2010 Contract No.: 1.
27 Mittal P, Dua S, Kalia V. Pictorial essay: Susceptibility-weighted imaging in cerebral ischemia2010.
28 Santhosh K, Kesavadas C, Thomas B, Gupta AK, Thamburaj K, Kapilamoorthy TR. Susceptibility weighted imaging: a new tool in magnetic resonance imaging of stroke. Clinical Radiology. 2009;64(1):74-83.
29 Hermier M, Nighoghossian N. Contribution of Susceptibility-Weighted Imaging to Acute Stroke Assessment. Stroke. 2004 August 1, 2004;35(8):1989-94.
30 Haacke EM, Makki M, Ge Y, Maheshwari M, Sehgal V, Hu J, et al. Characterizing iron deposition in multiple sclerosis lesions using susceptibility weighted imaging. Journal of Magnetic Resonance Imaging. 2009;29(3):537-44.
31 Niwa T, de Vries L, Benders M, Takahara T, Nikkels P, Groenendaal F. Punctate white matter lesions in infants: new insights using susceptibility-weighted imaging. Neuroradiology. 2011:1-11.
32 Vinod Desai S, Bindu PS, Ravishankar S, Jayakumar PN, Pal PK. Relaxation and susceptibility MRI characteristics in Hallervorden-Spatz syndrome. Journal of Magnetic Resonance Imaging. 2007;25(4):715-20.
33 Kirsch W, McAuley G, Holshouser B, Petersen F, Ayaz M, Vinters HV, et al. Serial susceptibility weighted MRI measures brain iron and microbleeds in dementia. Journal of Alzheimer's disease: JAD. 2009;17(3):599-609.

Contact

Jose Luis Ascencio L.
Escanografia Neurologica
Medellin
Colombia

jotaascencio@yahoo.com